ADAPTIVE MESH GENERATION FOR TCAD WITH GUARANTEED ERROR BOUNDS

René Heinzl[△]
Philipp Schwaha[△]
Michael Spevak[°]
Tibor Grasser[△]

[△]Christian Doppler Laboratory for TCAD in Microelectronics
at the Institute for Microelectronics

[°]Institute for Microelectronics, Technical University Vienna,
Gußhausstraße 27-29/E360, A-1040 Vienna, Austria
E-mail: {heinzl|schwaha|spevak|grasser}@iue.tuwien.ac.at

KEYWORDS
Mesh generation, error estimation, mesh quality

ABSTRACT

An adaptive three-dimensional mesh generation strategy is presented. In contrast to other work which is based on simple meshing techniques, we use advanced unstructured meshing techniques, driven by error estimators, to realize automatic adaptation and guarantee quality. The mesh optimization strategy is based on a classification scheme with a fuzzy indexing for the degree of degeneration of the elements. The applicability and usability of this complete automated process is presented with real-world examples.

INTRODUCTION

The methods employed in technology computer aided design (TCAD), such as finite differences, finite elements and, finite volumes, to calculate numerical solutions of partial differential equations require a suitable tiling of the simulation domain with simple elements. The tiling requries to fill the complete domain with no overlaps or no gaps. This tiling is called *tesselation*. The differential equations that need to be solved result from modeling a number of disparate physical phenomena such as dopant diffusion, mechanical deformation, heat transfer, fluid flow, electromagnetic wave propagation, and quantum effects. How suitable a given tessellation is depends not only on the type of equation, but also on the method employed to compute an approximate solution.
This transition from the continuous domain to a discretized domain or tessellation, commonly known as *mesh generation* [1], will inherently produce errors in the computed results, no matter how sophisticated or how appropriate a mathematical model is. This approximation error can be enormous, and can completely invalidate numerical predictions if no estimated or quantitative measure of these errors is available. The general subject is referred to as *a posteriori error estimation*.
To achieve a high confidence within simulations, all results have to stay with given error bounds. If these error bounds cannot be guaranteed, the mesh needs to be adapted. In two dimensions the user can supervise the generation of a mesh and even adjust its adaptation relatively easily. The transition from two to three dimensions virtually eliminates this possibility, as both visualization and user interaction are by far more difficult. As a result the user has little knowledge where to best adapt the mesh. Because of this it is essential for three-dimensional mesh generation and adaptation to work in conjunction with some kind of error estimator [2, 3] to make automatic generation and adaptation without user intervention possible. An automatic mesh optimization (mesh adaptation with a control criterion) procedure has to guarantee the quality of this automatic approach [4].

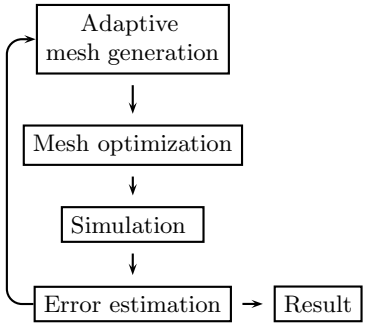

Figure 1: Principal flow of the adaptive mesh generation.

ADAPTIVE MESH GENERATION

When equipped with a measure for the error resulting from the chosen mesh, the question arises how to adapt the mesh in order to improve the accuracy of the calculated result. This question cannot be answered in a straight-forward manner due to the different requirements from TCAD.
On the one hand, process simulation requires boundary integrity, has to handle all kinds of degeneration for surface triangles (e.g. obtuse angles) in topography simulation, and has to generate surface and interface aligned elements for ion implantation and diffusion simulation.
Device simulation, on the other hand, with highly non-linear models requires a direction dependent mesh density and is very sensitive to the underlying mesh. Device simulation is normaly based on the finite-volume method. This method

needs consistent control volumes, called Voronoi regions. Therefore the mesh generator must generate the dual elements, the Delaunay elements.
The most promising mesh generation technique for three dimensions, the enhancement of the incremental Delaunay refinement algorithm to three-dimensions [5] (used in Tetgen [6]), has not yet found its way to all engineering applications due to the fact that a disregard for boundary integrity is the major drawback of this method.
Tree-based mesh generation methods cannot incorporate non-planar surfaces and in general produce a larger number of points than necessary. Inherently the generation of surface aligned refinement layers is not possible, although a lot of work has been done to avoid these disadvantages [7], boundary integrity is still not easily guaranteed. The quality of the elements is mostly predetermined by the tree discretization method and therefore limited to tetrahedra generated from a cube. On that account it has been proven for the two-dimensional [8] and the three-dimensional case [9] that no degenerated elements are generated.
Attempts of error estimation and adaptive mesh generation have already been undertaken exhibiting a highly increased rate of convergence in the sequencing simulation step in two dimensions [10]. The results for the three-dimensional case have not displayed this desirable trend. This is attributable in great part to the problems involved in mesh generation for the three-dimensional case.
The comprehensive mesh generation approach for TCAD [1] is ideally suited for the adaptive mesh generation part. Because of the advancing front all mesh generation parts can also be used for mesh adaption steps driven by a posteriori error estimators.

MESH OPTIMIZATION

To guarantee the quality during the adaptive mesh generation process, geometrical and topological optimization steps have to be performed. The definition of a quality measure for elements in three-dimensions is a relatively tedious task because of the consideration of quality with regard to the further use of the mesh. As an example a suitable mesh for topography simulation can never be useful for device simulation. Additionally a lot of different and conflicting quality measures for tetrahedra have been established [8, 11–13]. In addition most of the classification methods use only one of these quality measures like surface area, volume area, radius ratio, mean ratio, solid angle, dihedral angle, or edge ratio to classify the elements.
This is not without difficulty, as on the one hand, most degenerated elements (Figure 2) are not identifiable by a single quality measure. The *wedge* cannot be identified by the dihedral angle criterion or the *sliver* cannot be identified by the edge ratio. Especially in the area of TCAD some kind of degeneracy has to be allowed for special applications to reduce the number of points. In interconnect structures, for instance, a lot of *wedges* are used mostly for the coating elements. Then, the tetrahedra are classified by the number of degenerated triangles, like daggers and blades. The dagger has one short edge and at least one small angle, where the blade has no short edge and therefore one large and two small angles.
To allow this kind of freedom in the classification of quality a non-straight forward classification scheme is used and subdivided into two main parts similar to [12]. First, we identify four classes of quality defined by the number of small dihedral angles (Figure 2).

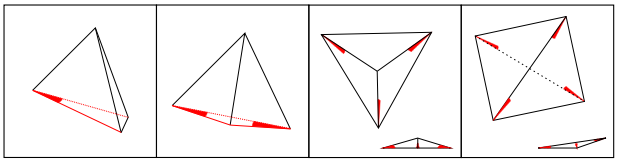

Figure 2: Four different classes of degenerated tetrahedra (wedge, spade, cap, sliver), sorted by the number of acute dihedral angles.

The needle (or spire) with three daggers (the short edges are marked in the figure), the slat (or splinter) with two opposite short edges and therefore four daggers, and the spindle with no short edges and therefore four blades as triangles is shown in Figure 3.

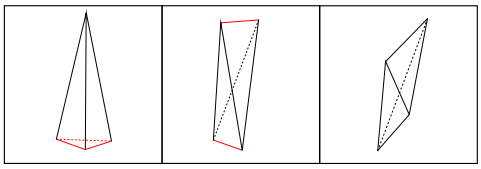

Figure 3: Three different types of degenerated tetrahedra (needle, slat, spindle).

Based on these two categories a fuzzy classification scheme for tetrahedra is derived. Fuzzy means, that the indexing for each type of degeneration is done by an adjustable threshold, whereas the threshold can be adjusted to the current application. The next diagram shows a typical example of a degenerated tetrahedron which belongs to more than one class of degeneration (the percent value reads for the classification amount).

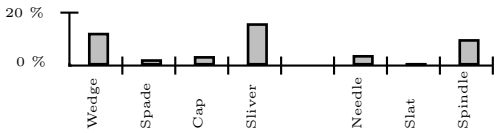

With the freedom in this classification scheme different types of optimization processes are customized for an application to achieve best results. In other words, we can easily search for a global quality optimum for specific tasks.
The following improvement techniques are used in our mesh optimization approach: vertex relocation [14], edge/face swapping, edge collapsing, and edge splitting. Results from different improvement techniques are shown in the next diagram. The initial mesh is generated without any geometrical or topological optimization strategy.

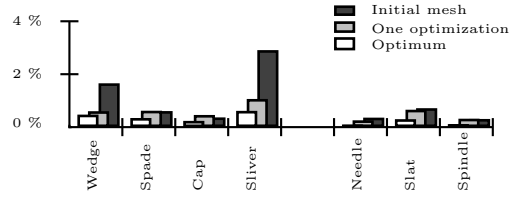

The reduction of all degenerated tetrahedra and particularly the most problematic *sliver* type within each optimization step can be clearly seen (the percentages read for the relative number compared to the total number of tetrahedra).
A real-world example from TCAD process simulation is selected to demonstrate the performance of the mesh optimization. Process simulation usually relies on the finite element method or the level set method where the Delaunay property is not necessary for the tessellation of the simulation domain. To emphasize the robustness of the optimization step the most challenging example in form of three-dimensional topography simulation is chosen. Starting from a base structure, in this case a realistic trench geometry, the surface is moved according to the level set method [15] in order to simulate an isotropic deposition procedure. Afterwards the new surface is extracted from the level set module and the surface mesh is subsequently adapted [16] in order to enhance the quality of the surface triangles and to reduce the number of mesh points. Next the new surface is merged with the original base structure and the resulting object is meshed. The final structure that results from the various optimization steps can be seen in Figure 4.

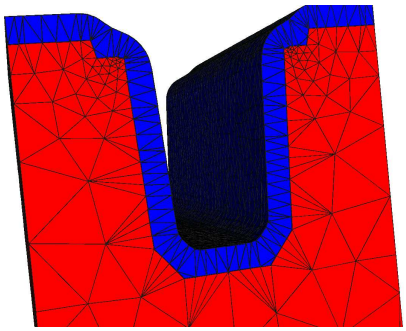

Figure 4: Isotropic deposition topography simulation of a realistic trench.

In the next diagram the result from the optimization strategy to reduce the degree of degeneration is presented. All different degeneration types are drastically lowered by the optimization steps.

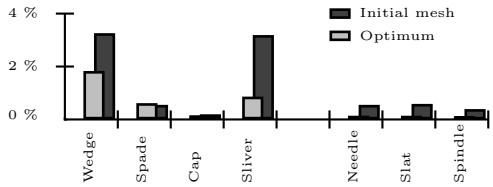

ERROR ESTIMATION

Discretization of the equations describing the problem is needed to make numerical treatment possible. The discretized problem then results in a discrete distribution of quantities and ansatz functions. The accuracy of the simulation does not solely depend on the quality of the underlying mesh but also on the suitability of the ansatz functions that have been chosen. The use of piecewise affine or constant ansatz functions, as in the case of finite elements or finite volumes, results in a certain characteristic of the error. In terms of function spaces a projection of the complete space

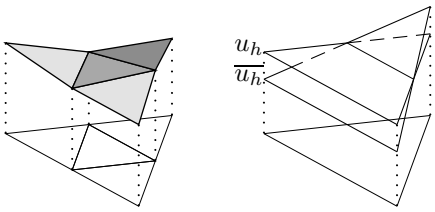

Figure 5: Left: Two-dimensional representation of the error estimator. The normal component of the error changes at the facet. Right: Discrete solution function u_h and the interpolation function $\overline{u_h}$ as function over the mesh triangle.

of functions to the subspace of the chosen ansatz functions is performed. The euclidean norm can then be used to measure the distance of two functions.

$$\|f-g\|_2 = \sqrt{\int_{-\infty}^{+\infty} \big(f(x)-g(x)\big)^2 \mathrm{d}x} \qquad (1)$$

Residual based error estimation

For a residual based error estimator (RS) a globally continuous function is constructed by piecewise affinely interpolating the computed numerical solution (Figure 5) for each triangle. The Laplace equation is satisfied exactly for the interior of the triangles but is discontinuous at the boundaries. This discontinuity of the interpolated function leads to an error that can be estimated locally by the following expression [17]:

$$\eta_K = h_K \Big(\sum_{E \in E_K \cap E_{\text{int}}} \|J_{E,n}\,(u_h)\,\|_E^2 + \sum_{E \in E_K} \|J_{E,t}\,(u_h)\,\|_E^2 \Big). \qquad (2)$$

Here, E_K denotes the edges of the triangle and E_{int} is the set of the interior edges. The two components of the sum are the normal component $J_{E,n}$ and the tangential component $J_{E,t}$ of the gradient $\vec{J_E}$ of the local discontinuity of the interpolated function. The geometry factor h_K marks a characteristic length of the triangle such as the mean edge length or the circumference radius.
Due to the use of piecewise affine interpolation the resulting function is continuous and hence the tangential component of the jump vanishes and only the normal component has to be considered.

ZZ Error Estimator

The ZZ error estimator [18] assumes the smoothness of the correct solution. A smoothed solution $\overline{u_h}$ (Figure 5) is calculated from the numerical solution u_h and then compared to the numerical solution. The difference of u_h and $\overline{u_h}$ is interpreted as a measure for the error in the solution u_h. The ZZ error estimator has been shown to have both an upper and a lower bound for certain types of differential equations such as the Laplace equation [18]. Polynomial functions of degree one in each tetrahedron have been chosen to obtain the smoothed solution. The distance between the interpolated piecewise affine function and the piecewise constant function can be determined by the evaluation of the norm presented in (1) and yields:

$$\eta_K = \sum_i U_i^2 - \sum_{i \neq j} U_i U_j, \qquad (3)$$

where the U_i are the resulting potential values at the vertices of the tetrahedron.

RESULTS

To demonstrate the overall behavior of the close interaction between all parts a realistic interconnect line with tapered line elements and pyramidal elements for the vias is used. Tapered means lines with angular side walls and the vias connect the two lines as shown in Figure 6. Afterwards the residual and the ZZ error estimation techniques are compared. The evolution of the quality of the tetrahedra during the mesh optimization process is also presented.

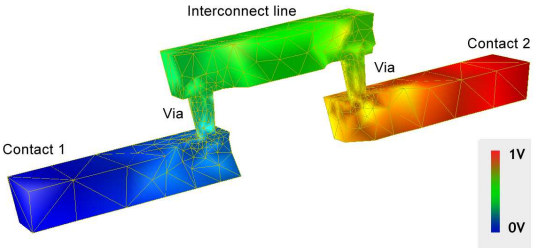

Figure 6: Initial structure with potential gradient.

The residual of each element is calculated by taking its neighboring elements into account, therefore the error estimates give a good indication where to adapt the mesh and the errors are reduced. This comes at the expense of computation time, which is twice that of the ZZ error estimator. As can be seen in the next diagram the error decreases due to the adaptation process, while keeping excellent overall mesh quality.

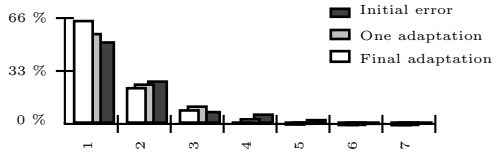

It is imperative for the following calculations that the *sliver* type is eliminated wherever possible. The distribution of mesh elements indicating the mesh quality based on the fuzzy classification scheme is presented next.

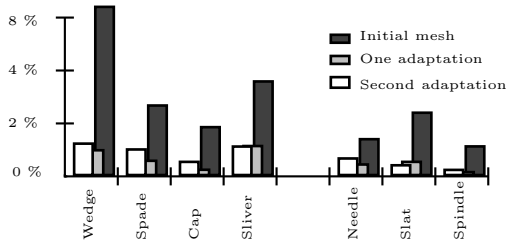

Due to the nature of the error estimators, a visualization has to take the fact into account, that error values are located on the highest dimensional object, in this case on tetrahedra. To give an impression of the estimated and improved error values a three-dimensional tetrahedra visualization is presented. The corresponding error values are mapped onto the tetrahedra with a so-called transfer function. The final visualized results are presented in the Figures 7 and 8. Again the reduction of error is clearly observable.

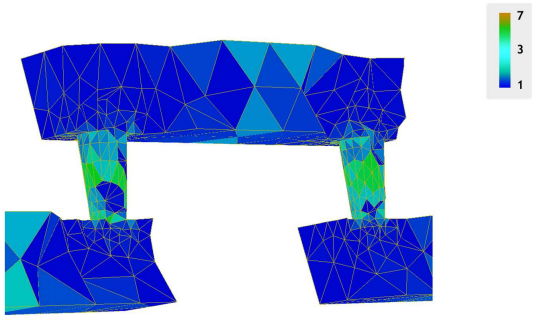

Figure 7: RS error estimation adaptive mesh refinement steps, initial error.

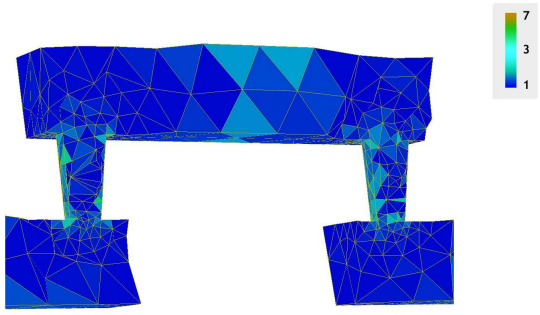

Figure 8: RS error estimation adaptive mesh refinement steps, last adaptation step.

The next diagram presents the distribution of the ZZ estimated error classes in the initial structure, after one adaptation step, and after a second adaptation step. The ZZ error estimation technique is by its design local and can therefore not include any information from the neighboring tetrahedra. Therefore this technique does not shift all elements to the lower error classes as quickly as the residual error estimation technique does.

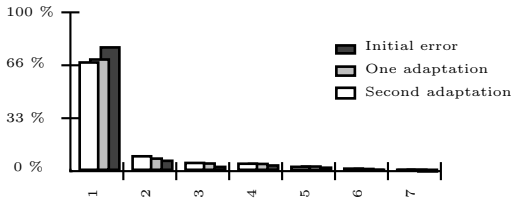

The next diagram presents the different steps of the mesh optimization strategy. The reduction of each degree of degeneration can be clearly observed.

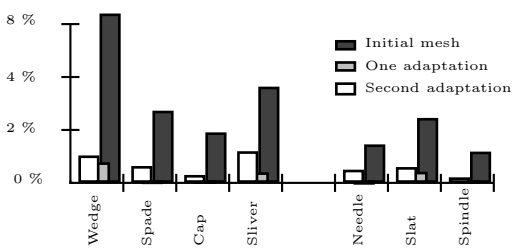

Finally the estimated ZZ error values are shown in Figures 9 and 10.

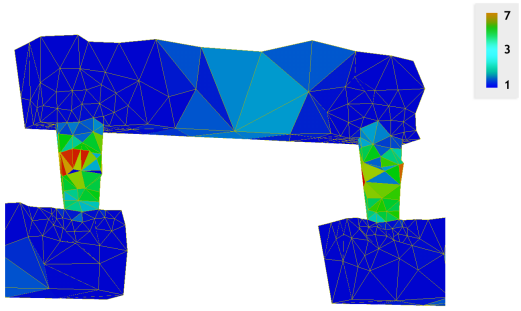

Figure 9: ZZ error estimation adaptive mesh refinement steps, initial error.

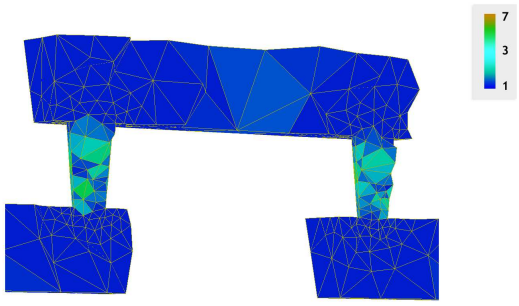

Figure 10: ZZ error estimation adaptive mesh refinement steps, last adaptation step.

CONCLUSION

The feasibility of coupling a posteriori error estimators to adaptive meshing has been presented. Utilizing recent advances in mesh generation it has become possible to considerably increase the quality of the simulation result while at the same time keeping the simulation time and required resources to a minimum. This is achieved by only refining areas corresponding to high error values using adaptively leading to an automatic adjustment of mesh density in sensitive areas. The ZZ error estimator is cheaper to compute compared to the residual error estimator, but also shows a lower rate of convergence. The overall mesh quality is guaranteed by the employed optimization scheme. With this complete flow the confidence in the simulation results can be given by bounding the errors in each step.

REFERENCES

[1] R. Heinzl and T. Grasser, in *Proc. SISPAD* (Kobe, Japan, 2005), pp. 211–214.

[2] J. Oden, ASME, USACM Standards (2002).

[3] S. Prudhomme, J. Oden, T. Westermann, and M. E. B. J.Bass, International Journal for Numerical Methods in Engineering **56**, 1193 (2003).

[4] R. Heinzl, M. Spevak, P. Schwaha, and T. Grasser, in *2005 PhD Research in Microelectronics and Electronics (PRIME 2005)* (IEEE, Lausanne, Switzerland, 2005), pp. 175–178.

[5] J. R. Shewchuk, Ph.D. thesis, School of Computer Science, Carnegie Mellon University, Pittsburgh, Pennsylvania, 1997.

[6] H. Si, *TetGen 1.3 User's Guide*, Weierstrass Institute for Applied Analysis and Stochastics, Germany, 2005, http://tetgen.berlios.de/.

[7] G. Garretón, Dissertation, ETH, Zürich, 1999.

[8] Bern and Eppstein, *Computing in Euclidean Geometry, World Scientific, Lecture Notes Series on Computing – Vol. 1* (1992).

[9] S. A. Mitchell and S. A. Vavasis, in *Symposium on Computational Geometry* (1992), pp. 212–221.

[10] L. Jänicke and A. Kost, IEEE Transactions on Magnetics **32**, 1334 (1996).

[11] T. Baker, in *Proc. 7th Int. Conf. Finite Element Methods in Flow Problems* (1989), pp. 1018–1024.

[12] S.-W. Cheng, T. K. Dey, E. A. Ramos, and T. Ray, in *SCG '04: Proc. 20th ASCG* (ACM Press, 2004), pp. 290–299.

[13] P. P. Pébay and T. J. Baker, Mathematics of Computation **72**, 1817 (2003).

[14] D. A. Field, Communications in Applied Numerical Methods, Wiley **4**, 709 (1988).

[15] A. Sheikholeslami *et al.*, in *Proc. ULIS* (IEEE, Bologna, Italy, 2005), pp. 139–142.

[16] A. Hössinger, J. Cervenka, and S. Selberherr, in *Proc. SISPAD* (Boston, USA, 2003), pp. 259–262.

[17] S. Nicaise, Université de Valenciennes et du Hainaut Cambrésis, MACS, ISTV, Valenciennes Cedex 9, France (2004).

[18] O. Zienkiewicz and J. Zhu, Int. J. Numer. Meth. Engrg. **24**, 337 (1987).

BIOGRAPHIES

RENÉ HEINZL studied electrical engineering at the TU Wien. He joined the Institute for Microelectronics in November 2003, where he is currently working on his doctoral degree. His research interests include process simulation, solid modeling, and adaptive mesh generation for TCAD with special emphasis on three-dimensional applications.

PHILIPP SCHWAHA studied electrical engineering at the TU Wien. He joined the Institute for Microelectronics in June 2004, where he is currently working on his doctoral degree. His research activities include circuit and device simulation, device modeling, and software development.

MICHAEL SPEVAK studied electrical engineering at the TU Wien. He joined the Institute for Microelectronics in December 2004, where he is currently working on his PhD.

TIBOR GRASSER is currently employed as an Associate Professor at the Institute for Microelectronics. In 2003 he was appointed head of the Christian Doppler Laboratory for TCAD in Microelectronics, an industry-funded research group embedded in the Institute for Microelectronics. His current scientific interests include circuit and device simulation and device modeling.